Electronic Supplementary Material (ESI) for Journal of Materials Chemistry C.

Supplementary Material (SM) for Enhanced vertical polarization and ultra-low polarization switching-barrier of two-dimensional SnS/SnSSe ferroelectric heterostructure

Yun-Qin Li, Xin-Yu Wang, Shi-Yu Zhu, Dai-Song Tang, Qi-Wen He, Xiao-Chun Wang*

Institute of Atomic and Molecular Physics, Jilin University, Changchun 130012, the People's Republic of China

Corresponding author: wangxiaochun@jlu.edu.cn

A. Construction process of SnS/SnSSe heterostructure

The construction process of SnS/SnSSe heterostructure can be simplified as follows[1]. In the first step, using the DFT-D3 method with the van der Waals correction[2, 3], the interlayer distance *d* has been varied and the total energy has been calculated with various interlayer distances. In the second step, SnS/SnSSe structure with the certain interlayer distance *d* (corresponding to the lowest energy) is used as the initial structure, and it is fully optimized under the condition of allowing complete relaxation of lattice and atomic positions. Next, the stability, polarization, polarization switching and electronic properties for the fully optimized SnS/SnSSe heterostructure are calculated.

B. Energy mutation aroused by structure mutation

We find that the mutation of energy for state IV (Fig. 1(b)) may be attributed by the structural mutation. In the optimized SnS/SnSSe heterostructure, neighboring-layer interaction is weaker than the interlayer interaction. The former refers to the interaction between SnS and SnSSe layers, and the later refers to the interaction between bonding atoms in both SnS and SnSSe layers. There is no bond between the two SnS and SnSSe layers due to the weaker neighboring-layer interaction. However, the application of external force will lengthen atomic bonds and weaken the interlayer interaction. Then, neighboring-layer interaction in SnS/SnSSe is stronger than the interlayer interaction.

Under the stronger neighboring-layer interaction, therefore, the SnS/SnSSe structure is mutated, leading to the two SnS and SnSSe monolayers combined with each other to form a five-layers structure (Sn atoms of SnS layer bond with the Se atoms of SnSSe layer), and resulting in the energy mutation. In Fig. 1(c), the distance *d* between Sn atoms of SnS and Se atoms of SnSSe layers is reduced from 3.262 Å (in state IV) to 1.194 Å (in mutated state), and the total energy is jumped from -21.856 eV to -21.952 eV. In addition, the phonon spectrum with obvious imaginary frequency at K point demonstrates the instability of the mutant state.

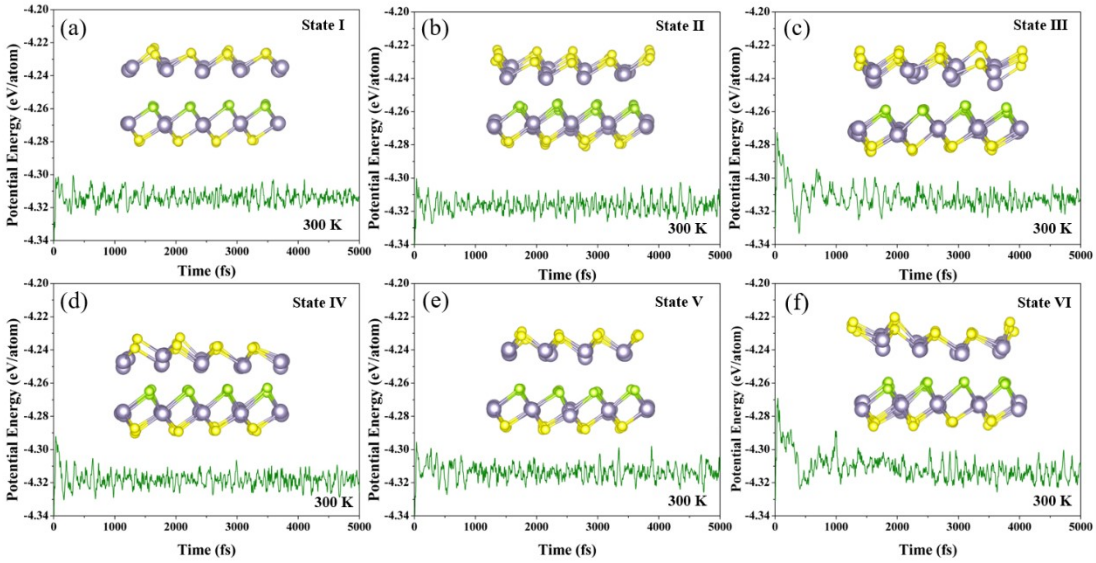

Fig. S1 The ab initio molecular dynamics (AIMD) simulation for SnS/SnSSe heterostructure with six stacking states.

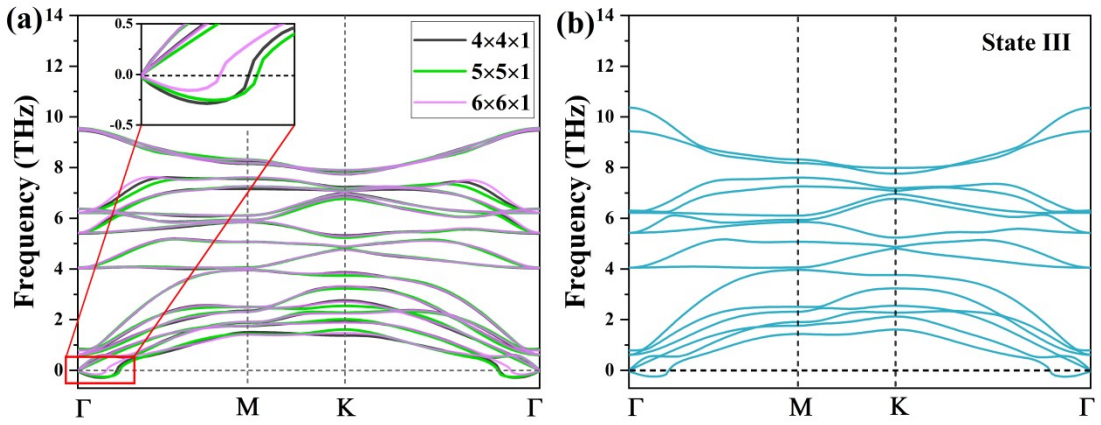

Fig. S2 (a) The phono spectra calculated by 4 × 4 × 1, 5 × 5 × 1 and 6 × 6 × 1 supercells

of the ground state for SnS/SnSSe heterostructure, the red box is in amplified, and (b) Phono spectra calculated by a 6 × 6 × 1 supercell of the stacking state III for SnS/SnSSe heterostructure.

C. Poisson's ratio v(θ) of SnS/SnSSe heterostructure.

To analysis the structural response of external strain, the square cell is constructed, which can facilitate the application of external strain on the SnS/SnSSe heterostructure. For state II, the optimized lattice constant a = 3.786 Å of its square cell (insets in the Fig. S4) is equal to that of its oblique cell, and the lattice constant b is equal to 6.557 Å. The -0.5 to +0.5% external compressive and tensile strain is applied along b-axis in the square cell. As shown in Fig. S4, when 0.1% compressive or tensile strain is applied, the structural lattice constant a has no obvious change. This may lead to the tiny negative calue of Poisson's ratio when we directly calculate the mechanical properties using its primitive cell. Therefore, we use the 2×2×1 supercell (Fig. S4) of SnS/SnSSe heterostructure to calculate the more accurate mechanical properties. The calculation results show that all states of SnS/SnSSe show positive Poisson's ratio.

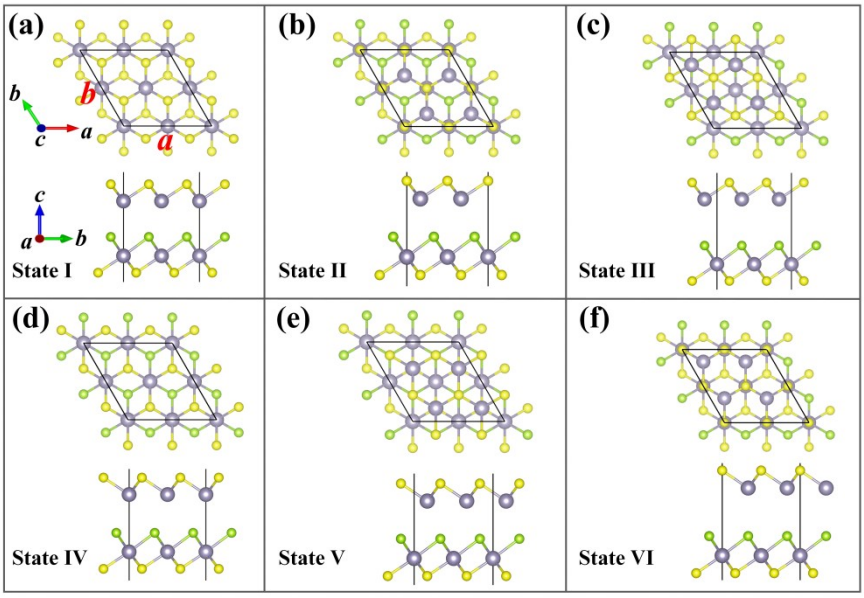

Fig. S3 The top and side views of the 2×2×1 supercell for SnS/SnSSe heterostructure with six stacking states I -VI.

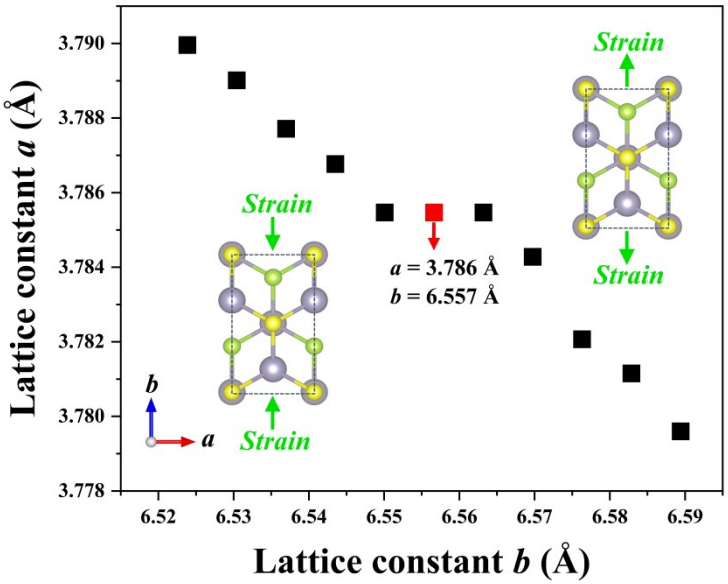

Fig. S4 Lattice constants *a* as a function of external compressive and tensile strain along *b*-axis direction the stacking state II for SnS/SnSSe heterostructure. Insets are the top views of a square cell for state II.

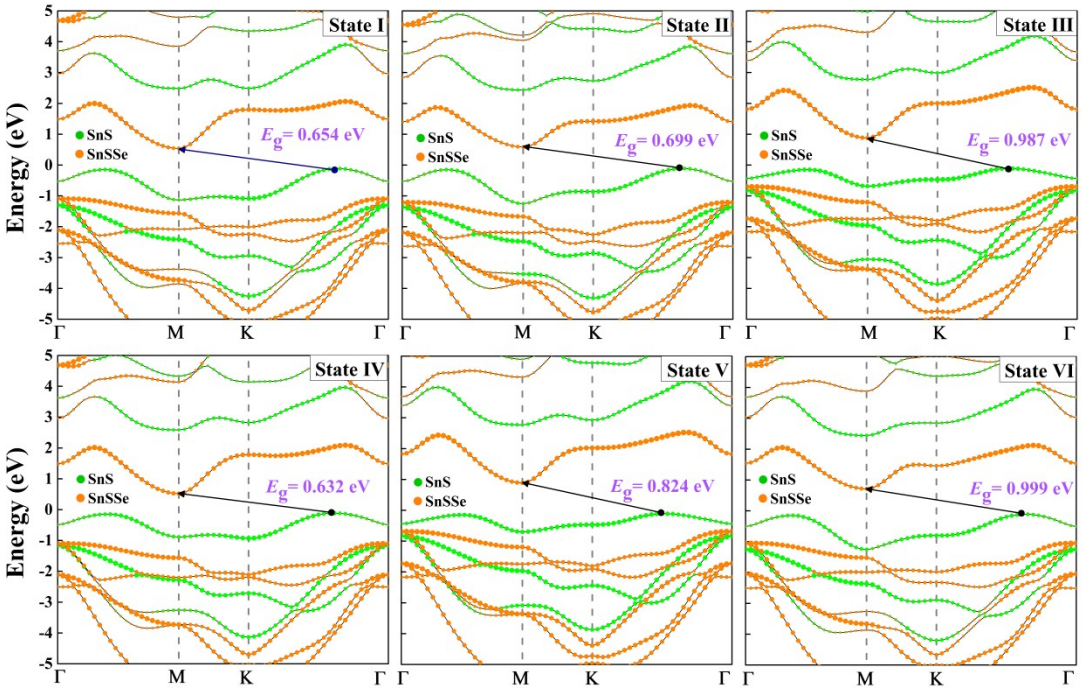

Fig. S5 Band structures based on the HSE06 functional for SnS/SnSSe heterostructure with six stacking states.

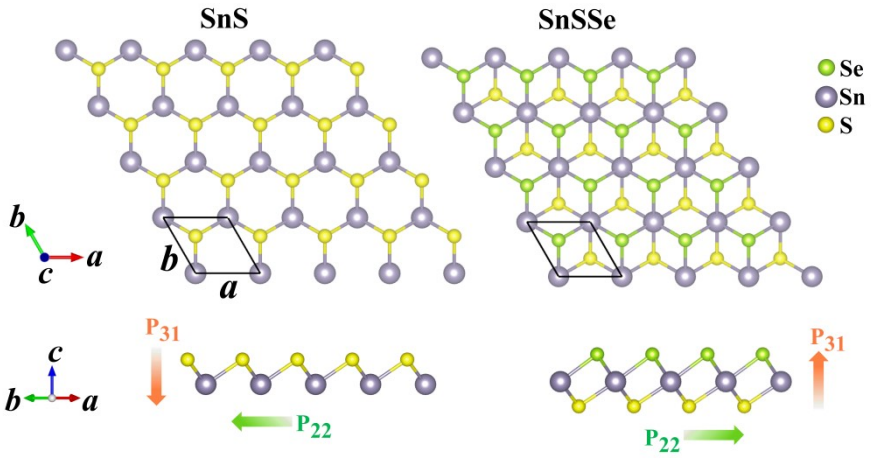

Fig. S6 Top and side views of SnS (left) and SnSSe (right) monolayers, $\mathbf{P_{22}}$ and $\mathbf{P_{31}}$ represent the in-plane and vertical polarizations.

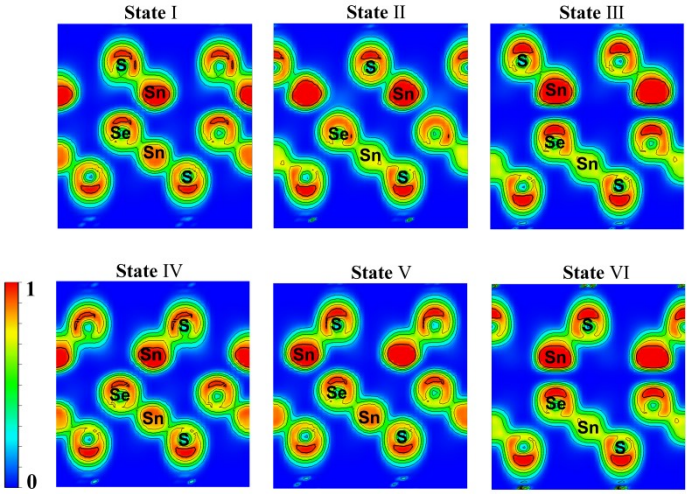

Fig. S7 The electron localization function (ELF) distribution for SnS/SnSSe heterostructure with six stacking states.

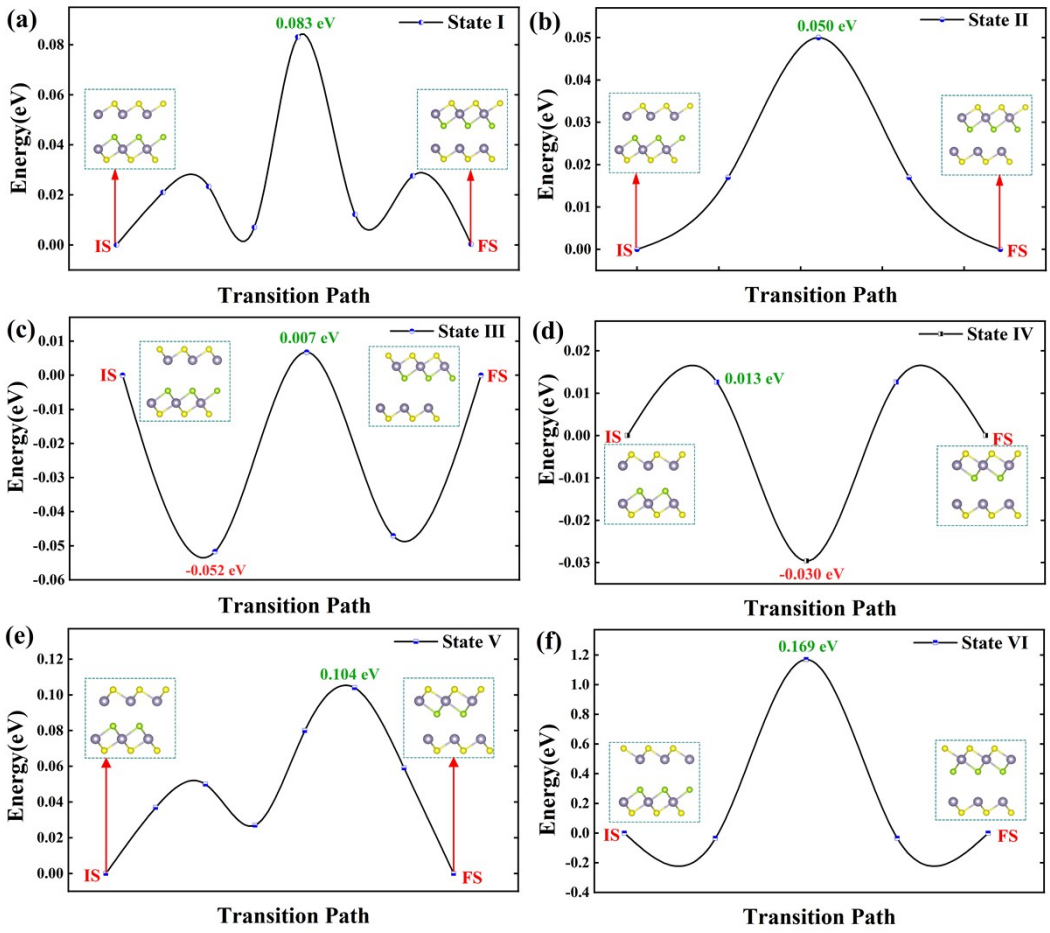

Fig. S8 Polarization switching pathways with energy barriers for six stacking states from SnS/SnSSe to SnSSe/SnS.

REFERENCES

1. M. K. Mohanta, A. Rawat, Dimple, N. Jena, R. Ahammed and A. De Sarkar, *Nanoscale*, 2019, **11**, 21880-21890.

2. S. Grimme, J. Antony, S. Ehrlich and H. Krieg, *The Journal of Chemical Physics*, 2010, **132**, 154104.

3. S. Grimme, S. Ehrlich and L. Goerigk, *Journal of Computational Chemistry*, 2011, **32**, 1456-1465.